Supporting Information:

Oral administration and detection of a near-infrared molecular imaging agent in an orthotopic mouse model for breast cancer screening

Authors: Sumit Bhatnagar[1], Kirti Dhingra Verma[1], Yongjun Hu[2], Eshita Khera[1], Aaron Priluck[1], David E. Smith[2], and Greg M. Thurber[1,3,*]

Affiliations:

[1] Department of Chemical Engineering, University of Michigan, Ann Arbor, MI 48109.

[2] Department of Pharmaceutical Sciences, University of Michigan, Ann Arbor, MI 48109.

[3] Department of Biomedical Engineering, University of Michigan, Ann Arbor, MI 48109.

* Corresponding author:

Greg M. Thurber
Email: gthurber@umich.edu
2800 Plymouth Rd.
Ann Arbor, MI 48109
T: 734-764-8722

Fig. S1

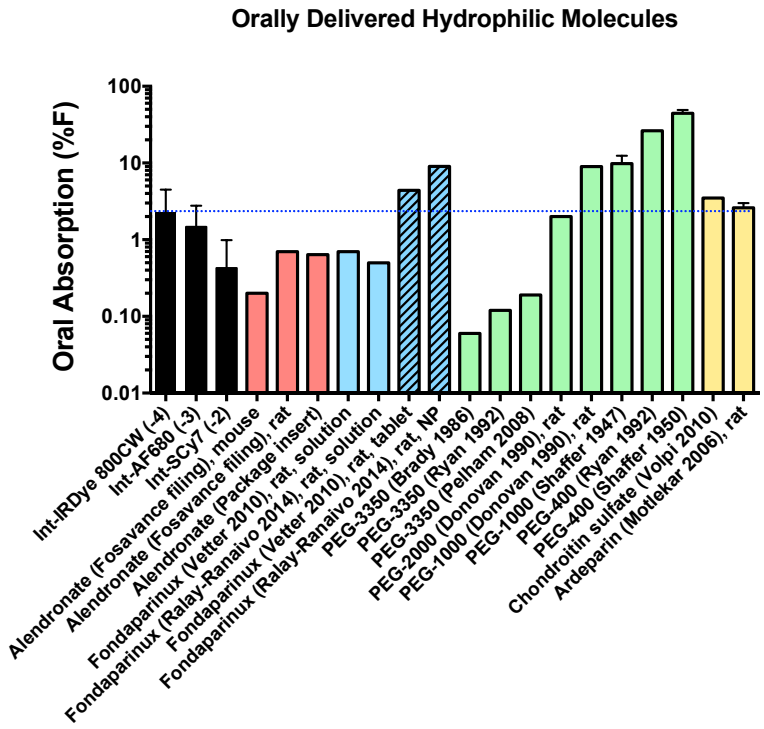

Figure S1. Oral Absorption of Select Hydrophilic and Anionic Molecules. The oral absorption of several hydrophilic molecules is shown. The 3 agents reported here (black) are within the range of reported clinical and animal studies. Alendronate (-2 charge, 249 Da) has lower absorption. Fondaparinux is a charged oligosaccharide with -10 charge and MW = 1728 and low absorption (light blue). When formulated to reduce pH and enzymatic degradation, much higher rates of absorption can be achieved (hatched light blue). Uncharged PEG (green) has lower absorption with larger molecular weight (3350 Da) than the imaging agents in this work, similar absorption around the same size, and higher absorption with lower molecular weight. This is unexpected, since anionic charges typically reduce absorption. However, the anions may contribute to improved absorption (while still low compared to lipophilic small molecule drugs) since larger anions (chondroitin sulfate, a polydisperse anionic polymer, MW = ~21 kDa[1] and ardeparin, average MW = 6 kDa, range 2-15 kDa) have been reported with similar absorption (yellow).

Extensive research has been conducted into increasing the oral absorption of macromolecules. These investigations include polyanionic agents such as chondroitin sulfate[2], unfractionated heparins[3], anionic dendrimers[4-6], and anionic formulations to improve absorption of these and other compounds[7-12]. Figure S1 below shows the oral absorption of several hydrophilic molecules (clinical data unless otherwise stated) in comparison with the current probes[13-22].

Some evidence suggests that these polyanionic molecules can modulate tight junctions to increase paracellular transport[11]. Polyanions, such as heparin, have also been shown to modulate tight junctions in other epithelial tissues such as the lung[23].

Hepatobiliary excretion

In addition to absorption, metabolism and/or excretion within the GI tract and liver (first-pass metabolism) can greatly impact systemic distribution following oral delivery. The low molecular weight heparin, fondaparinux, is degraded within the GI tract, likely resulting in the higher absorption following formulation as a tablet or nanoparticle[13, 14]. Similarly, charged dyes like ICG and some asymmetric cyanine dyes can undergo significant hepatobiliary excretion[24, 25], making these agents unsuitable for oral delivery.

Fig. S2

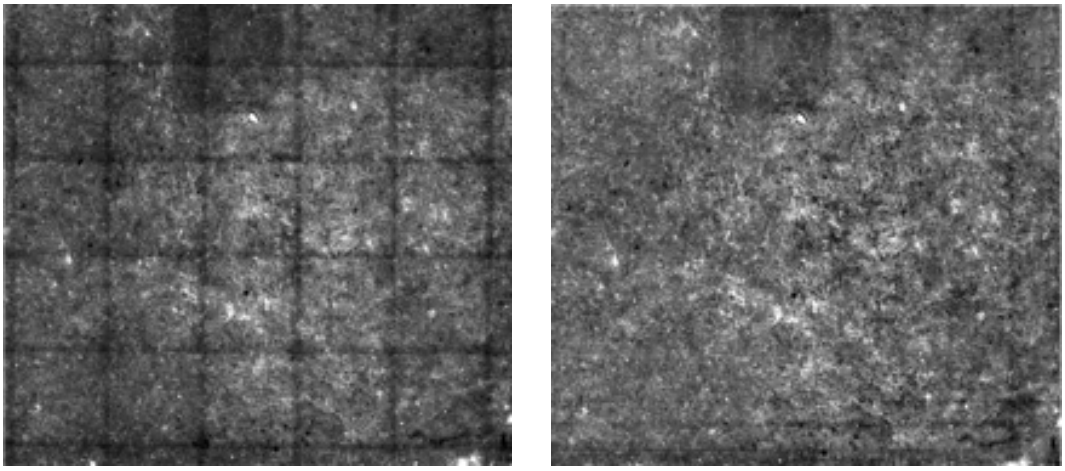

Figure S2. Image processing of confocal microscopy results. The integrin image had stitching artifacts. (Left) Confocal image of integrin expression in an MDA-MB-231 histology slide with stitching artifacts. (Right) Removal of artifacts using a FFT bandpass filter.

To overlay the Odyssey CLx image with the confocal microscopy images, the pixel size was matched, and the images were aligned using the tumor edge. The high resolution mac3 stain was processed using a 10 pixel Gaussian blur to match the resolution of the Odyssey CLx image (for overlay only).

Fig. S3

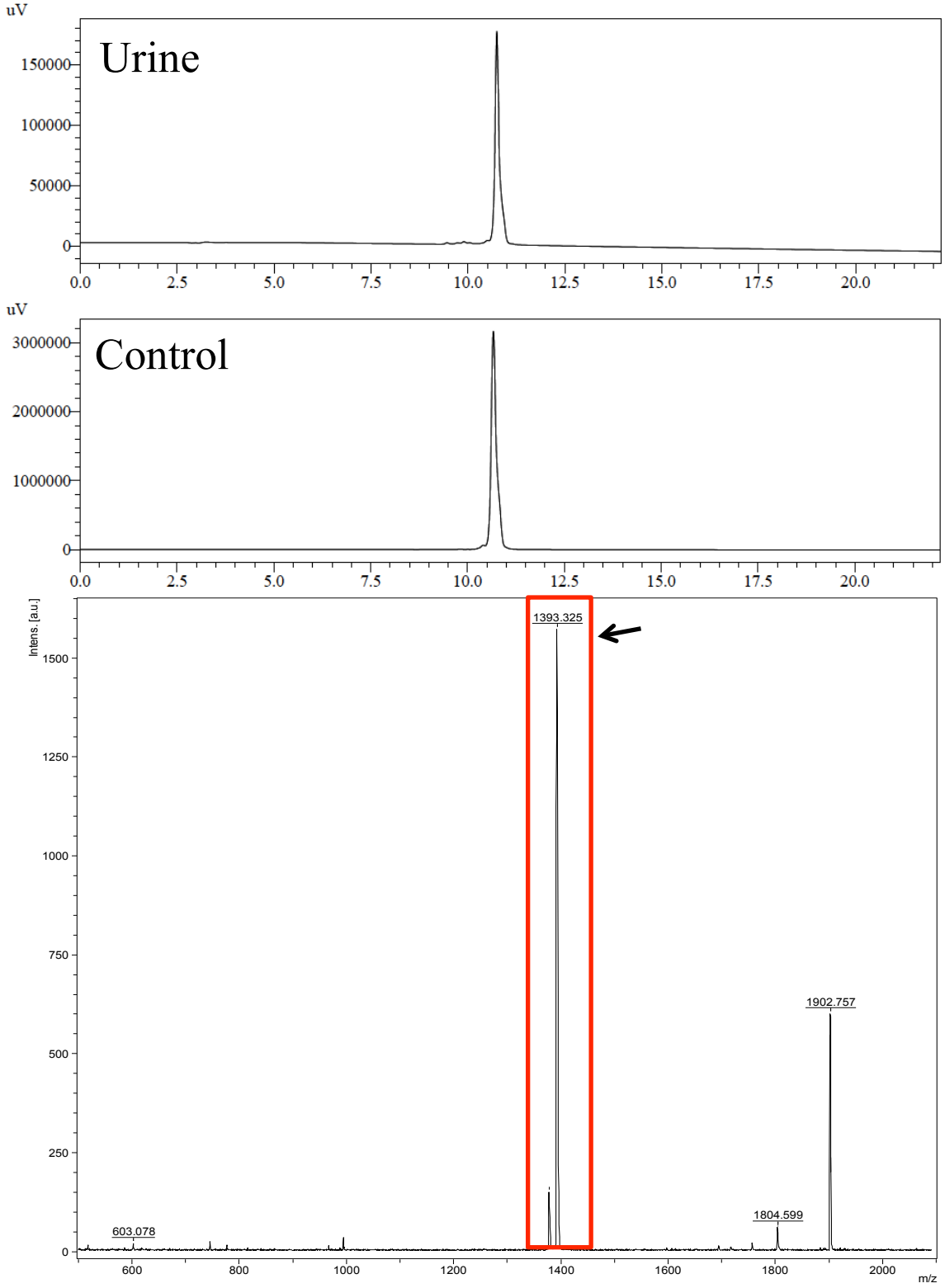

Figure S3. MALDI of a urine sample showing the IRDye800CW agent.

A 10-week old female C57BL/6 mouse was dosed with 5 mg/kg of the IRDye800CW agent and placed in a metabolic cage for a period of 24 hours. The urine from this mouse was collected and run on an analytical C18 column on a Shimadzu reverse phase HPLC. Absorption at 770 nm was used as the detection method with the dominant peak from the urine (top) matching a control injection of the intact probe (middle). The resulting peak was collected and run on MALDI, showing the molecular weight of the IRDye800CW Agent in the urine (bottom). Peaks with molecular weight 603 and 1804 were present in a negative control (urine collected from mouse that was not dosed with the imaging agent). The urine sample was also run on a native gel and SDS-PAGE and appeared as a single fluorescent band on both gels.

Fig. S4

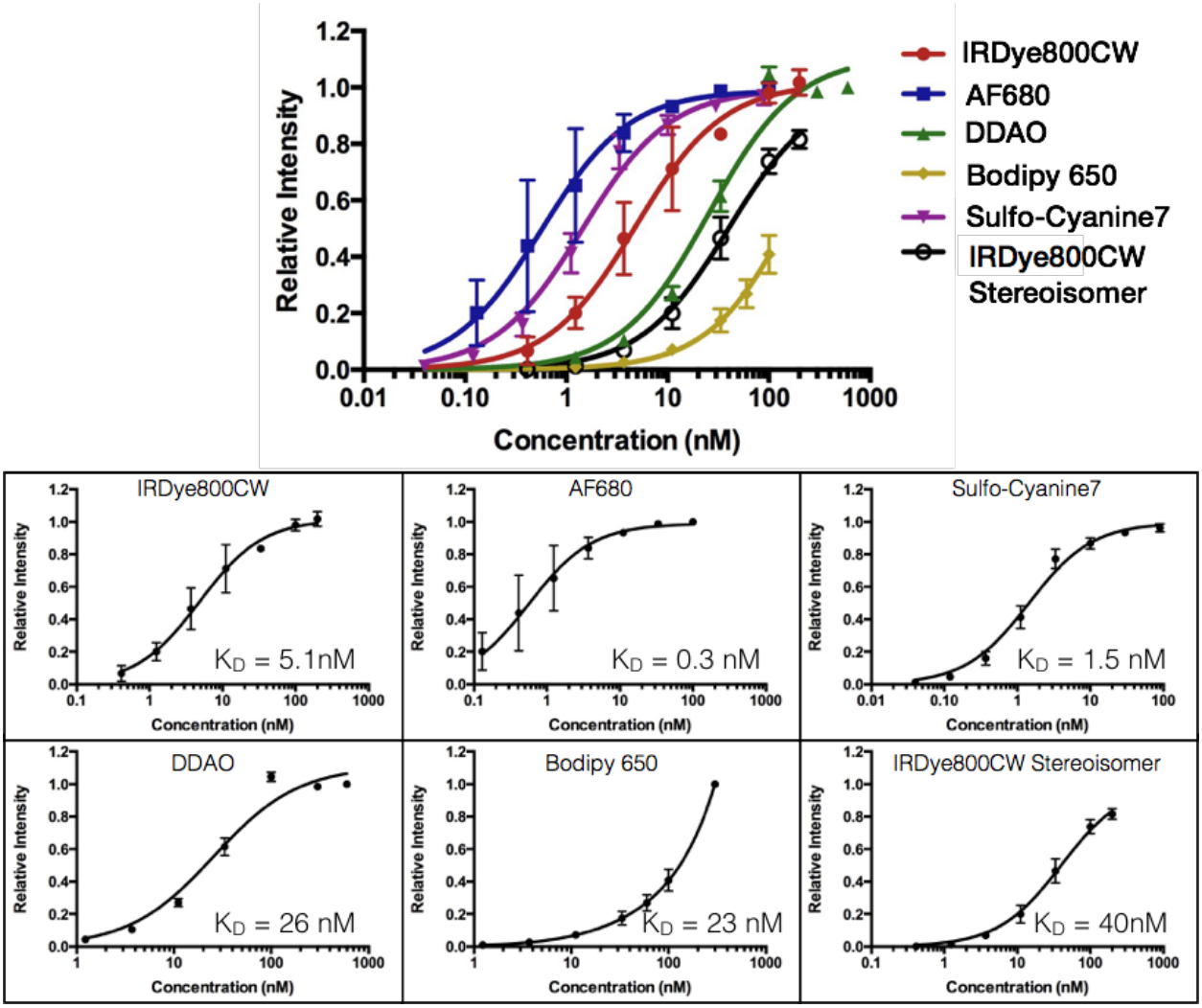

Figure S4. Binding affinity curves for all imaging agents. The highly lipophilic nature of the Bodipy650 agent made it difficult to experimentally differentiate specific binding from non-specific sticking. In order to calculate the binding affinity for this agent, the data was fit to a one-site specific binding equation in Graphpad Prism, with the addition of a non-specific binding term to the equation.

One Site Specific Binding Equation: $Y = \frac{Bmax*X}{X+K_D}$

where, Y is the relative intensity, X is the concentration and K_D is the binding affinity.

One Site Specific Binding with Non-Specific Binding Equation: $Y = \frac{Bmax*X}{X+K_D} + Cmax * X$

where, Cmax is the non-specific binding coefficient.

Fig. S5

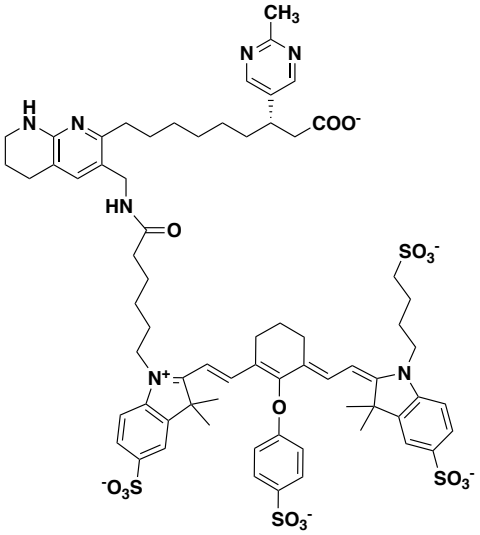

IRDye800CW Agent

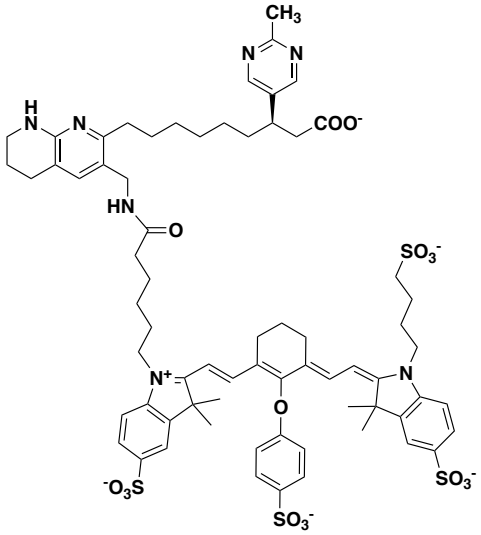

IRDye800CW Agent Stereoisomer

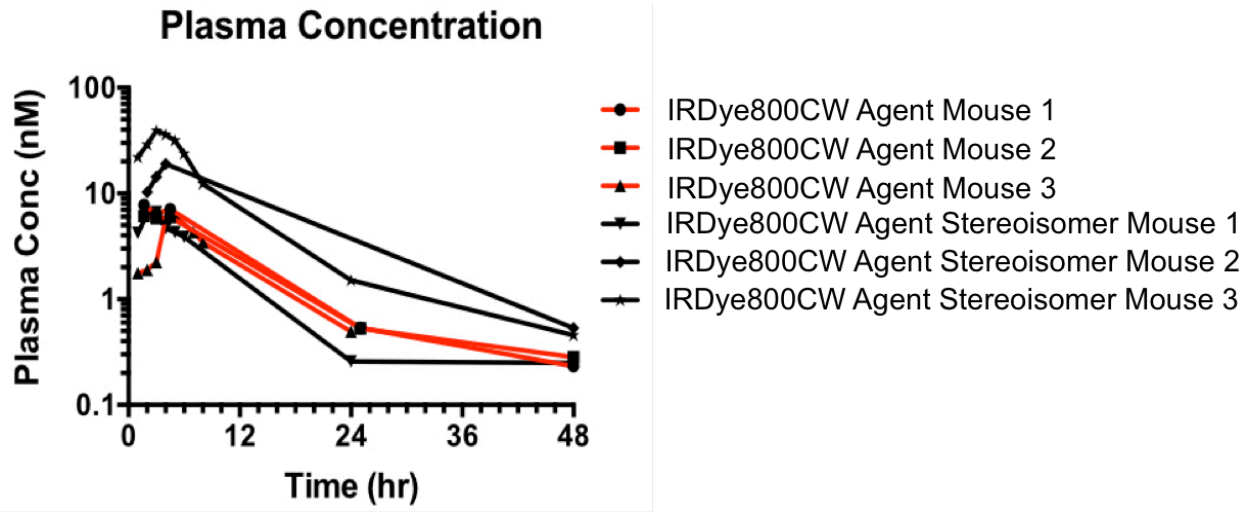

Figure S5. Structures of the IRDye800CW agent and its stereoisomer along with plasma clearance from mice with oral administration of both agents.

Fig. S6

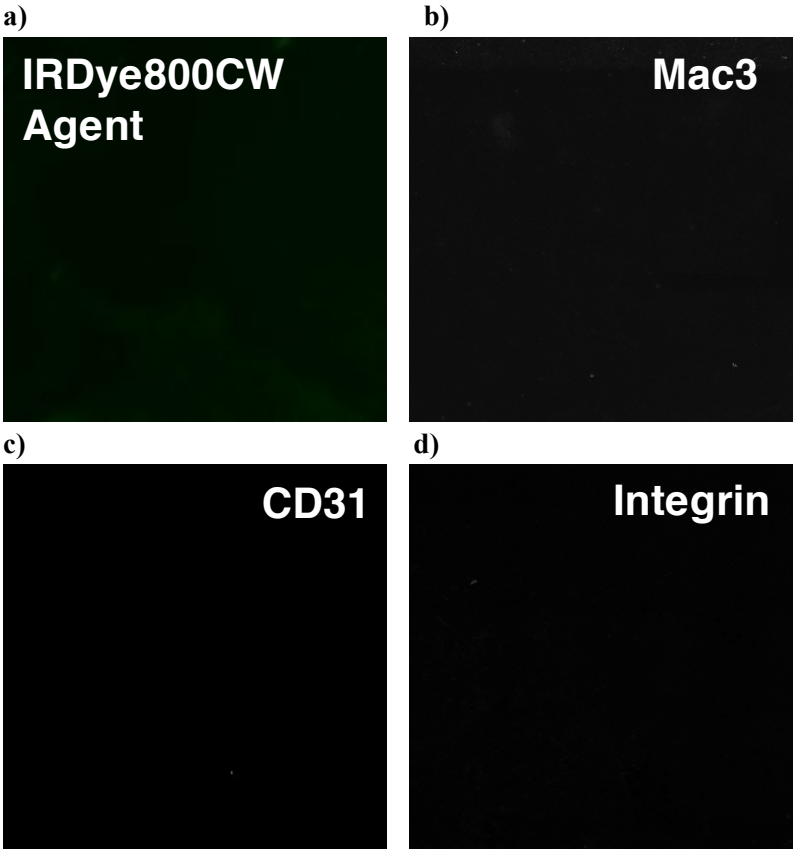

Figure S6. Negative control images of histology slides with no probe or ex-vivo labeling and same window leveling as Fig. 4 for a) IRDye800CW agent, b) Mac3, c) CD31 and d) integrin.

Fig. S7.

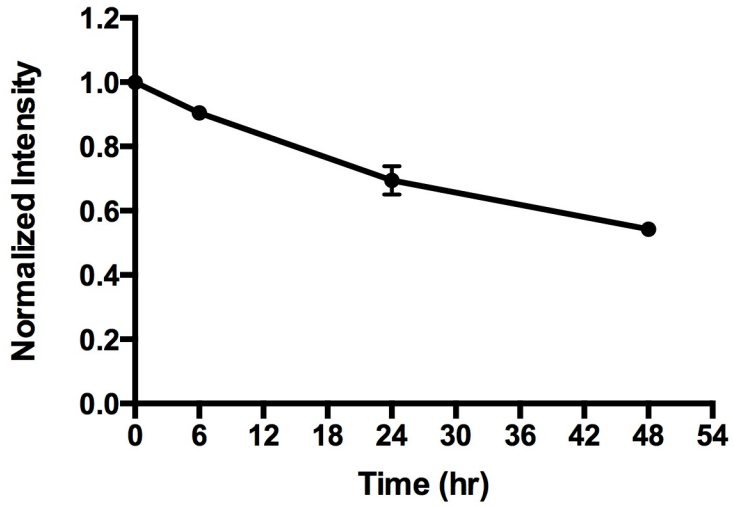

Figure S7. IRDye800CW agent serum stability over a period of 48 hours.

The agent was incubated in fetal bovine serum at 37°C and the fluorescence was measured at 6, 24 and 48 hours on the Odyssey CLx. The signals were normalized to the initial intensity. The imaging agent shows about a 45% decrease in signal over a period of 48 hours. Fig 3C shows that the fluorescent intensity in the tumor is relatively constant after 6 hours, indicating that the targeting of the tumor takes place in this time frame, where the stability of the agent only drops by 8% in serum.

Table S1 Clinical breast imaging studies

Contrast Agent	Tumor size	Contrast	Ref
ICG	~1 cm	(absorption)	[26]
ICG	1.5, 1.6, and 2.5 cm	3.5 to 5.5	[27]
ICG	1.6 and 1.1 cm	1.5 to 1.8	[28]
Omocyanine	2.9, 1.8, 2.4, 7.4, 3.4 cm	1.8 to 2.8	[29]
ICG	2.5 cm (mean), range 1.1 to 5.2 cm	0.25 to 0.64	[30]

Several clinical studies have demonstrated the feasibility of imaging breast tumors deep within breast tissue. These studies have primarily used indocyanine green (ICG), which is a non-targeted contrast agent that is approved by the FDA[26, 27, 30].

Probing breast tissue using light (diaphanography) dates back to the 1920's but made substantial advances in the late 1990's and early 2000's due to improvements in imaging equipment and tomographic techniques[31]. Corlu et al. was the first to publish fluorescence imaging of human breast tumors using ICG. The fluorescence imaging gave the best contrast, and other studies have indicated that fluorescence is better than absorption with low background concentrations[32]. Despite the promising results found in several trials, untargeted contrast agents do not perform better than mammography alone[33], and there is a strong need for targeted contrast agents[29].

Many additional studies have tested the limits of detection both theoretically and with optical phantoms. Tumors less than 2 cm[34] can be detected in the contrast ranges achieved here in mice, and the absolute concentrations of IRDye800CW are much higher than those detected using a clinical breast imaging system[35], indicating the contrast achieved with these orally delivered agents is suitable for clinical detection.

Table S2. Target and Ligand Selection Initial Design Criteria

	Criteria	Rationale
Target Selection (Integrin)	Extracellular target	Easily accessible from blood and rapid washout of unbound probe
	High expression in several cell types (tumor cells, macrophages and activated endothelium)	Robust detection for screening and sensitivity with NIR imaging[36]
	Internalizes probe at a significant rate	Lowers the required affinity[37]
	Well studied ligands against target	Circumvent the molecular screening step
Ligand Selection (Peptidomimetic)	Low molecular weight	Increase the oral absorption
	High stability	Prevent protease and/or acid degradation in GI tract to increase oral absorption
	Low toxicity	Maintain large safety margin for screening potentially healthy patients
	Low first pass metabolism	Low liver uptake/metabolism to increase oral absorption
	High affinity, maintained after conjugation with fluorophores	Enable efficient and specific targeting even with variable plasma concentrations

The above criteria were selected for our proof-of-concept studies. While not all these criteria are necessary for developing orally administered molecular imaging agents, they were used to provide the highest chance of success in the shortest development time.

Transport analysis indicates these molecules are likely binding-site and internalization limited[38] meaning that reducing protein binding/colloidal interactions is not as important as permeability surface area product (PS/V) limited agents. Plasma protein binding also impacts systemic clearance rates, which determines the absolute uptake in target and non-target tissues. Because the background signal from these probes is close to autofluorescence, a reduction in total signal may lower the target signal while the background does not decrease significantly (because it is dominated by tissue autofluorescence), thereby lowering the target to background ratio. Therefore, plasma protein binding in this scenario increases the contrast.

Table S3. Integrin expression levels on various cell types

	Expression level (receptors/cell)	Refs
Activated endothelium	$1.7x10^5$	[39]
Macrophages	$2x10^5$	[40]
Tumor cells	~$5\text{-}10x10^4$	[41, 42]

The molecular imaging field is actively engaged in pursuing new molecular targets or combinations of existing targets to continually improve the sensitivity, specificity, correlation with aggressiveness, identification of sensitivity to certain therapies (e.g. anti-HER2 therapy), and treatment response of cancer. Ultimately, the utility of any approach (target, modality, etc.) will need to be determined in clinical trials. However, clinical data looking at target expression and results from clinical trials with radiolabeled probes can provide some validation for target selection.

Table S4. Purification methods and purity of the final product

Agent	Mobile Phase	HPLC Method	Retention Time	Expected MW	Observed MW	Purity
IRDy800CW (High Affinity)	A: 25mM TEAA in water B: MeCN	25% B 0-6 min, 25-45% B 6-24 min	14 min	1397.682	1395.922	95%
AF680	A: 0.1% TFA in water B: 0.1% TFA in MeCN	5-30% B 0-12 min, 30-60% B 12-16min	13.25 min	1253.351	1253.314	96.5%
Sulfo-Cyanine7	A: 25mM TEAA in water B: MeCN	15-60% B 0-20 min	15 min	1103.405	1104.727	88%
DDAO	A: 0.1% TFA in water B: 0.1% TFA in MeCN	20-95% B 0-15 min	9.75 min	800.8	796.8	92%
Bodipy 650	A: 0.1% TFA in water B: 0.1% TFA in MeCN	20-95% B 0-15 min, 95% B Hold 15-16 min	11.5 min	938.9	940.1	87.5%
IRDye800CW Stereoisomer (Low Affinity)	A: 25mM TEAA in water B: MeCN	25% B 0-6 min, 25-45% B 6-24 min	14 min	1397.682	1399.260	97.4%

The imaging agents used in the study were purified on a a preparative scale Luna C18(2) column (Phenomenex; Torrance, CA) on a Shimadzu reverse phase HPLC according to the methods stated below in Table S5. The system used a flow rate of 10 ml/min and used absorbance to detect the samples either at 254nm or at the excitation maxima (Fig 1) of the respective fluorophore. Mass spectrometry was used to confirm conjugation of the targeting ligand with the fluorophores and a purity check was performed to show that there was no unconjugated fluorophores or other reactants in the final product

References:

1. Volpi, N. Analytical aspects of pharmaceutical grade chondroitin sulfates. *J Pharm Sci* **2007,** *96*, (12), 3168-80.
2. Xiao, Y.; Li, P.; Cheng, Y.; Zhang, X.; Sheng, J.; Wang, D.; Li, J.; Zhang, Q.; Zhong, C.; Cao, R.; Wang, F. Enhancing the intestinal absorption of low molecular weight chondroitin sulfate by conjugation with alpha-linolenic acid and the transport mechanism of the conjugates. *Int J Pharm* **2014,** *465*, (1-2), 143-58.
3. Hiebert, L. M.; Wice, S. M.; Ping, T. Increased plasma anti-Xa activity and recovery of heparin from urine suggest absorption of orally administered unfractionated heparin in human subjects. *The Journal of laboratory and clinical medicine* **2005,** *145*, (3), 151-5.
4. El-Sayed, M.; Ginski, M.; Rhodes, C.; Ghandehari, H. Transepithelial transport of poly(amidoamine) dendrimers across Caco-2 cell monolayers. *Journal of controlled release : official journal of the Controlled Release Society* **2002,** *81*, (3), 355-65.
5. Hubbard, D.; Enda, M.; Bond, T.; Moghaddam, S. P.; Conarton, J.; Scaife, C.; Volckmann, E.; Ghandehari, H. Transepithelial Transport of PAMAM Dendrimers Across Isolated Human Intestinal Tissue. *Mol Pharm* **2015,** *12*, (11), 4099-107.
6. Thiagarajan, G.; Sadekar, S.; Greish, K.; Ray, A.; Ghandehari, H. Evidence of oral translocation of anionic G6.5 dendrimers in mice. *Mol Pharm* **2013,** *10*, (3), 988-98.
7. Mousa, S. A.; Zhang, F.; Aljada, A.; Chaturvedi, S.; Takieddin, M.; Zhang, H.; Chi, L.; Castelli, M. C.; Friedman, K.; Goldberg, M. M.; Linhardt, R. J. Pharmacokinetics and pharmacodynamics of oral heparin solid dosage form in healthy human subjects. *Journal of clinical pharmacology* **2007,** *47*, (12), 1508-20.
8. Baughman, R. A.; Kapoor, S. C.; Agarwal, R. K.; Kisicki, J.; Catella-Lawson, F.; FitzGerald, G. A. Oral delivery of anticoagulant doses of heparin. A randomized, double-blind, controlled study in humans. *Circulation* **1998,** *98*, (16), 1610-5.
9. Castelli, M. C.; Wong, D. F.; Friedman, K.; Riley, M. G. Pharmacokinetics of oral cyanocobalamin formulated with sodium N-[8-(2-hydroxybenzoyl)amino]caprylate (SNAC): an open-label, randomized, single-dose, parallel-group study in healthy male subjects. *Clin Ther* **2011,** *33*, (7), 934-45.
10. Aungst, B. J. Absorption enhancers: applications and advances. *The AAPS journal* **2012,** *14*, (1), 10-8.
11. Maher, S.; Leonard, T. W.; Jacobsen, J.; Brayden, D. J. Safety and efficacy of sodium caprate in promoting oral drug absorption: from in vitro to the clinic. *Adv Drug Deliv Rev* **2009,** *61*, (15), 1427-49.
12. Walsh, E. G.; Adamczyk, B. E.; Chalasani, K. B.; Maher, S.; O'Toole, E. B.; Fox, J. S.; Leonard, T. W.; Brayden, D. J. Oral delivery of macromolecules: rationale underpinning Gastrointestinal Permeation Enhancement Technology (GIPET). *Therapeutic delivery* **2011,** *2*, (12), 1595-610.
13. Vetter, A.; Perera, G.; Leithner, K.; Klima, G.; Bernkop-Schnurch, A. Development and in vivo bioavailability study of an oral fondaparinux delivery system. *European journal of pharmaceutical sciences : official journal of the European Federation for Pharmaceutical Sciences* **2010,** *41*, (3-4), 489-97.
14. Ralay-Ranaivo, B.; Desmaele, D.; Bianchini, E. P.; Lepeltier, E.; Bourgaux, C.; Borgel, D.; Pouget, T.; Tranchant, J. F.; Couvreur, P.; Gref, R. Novel self assembling nanoparticles for the oral administration of fondaparinux: synthesis, characterization and in vivo evaluation. *Journal of controlled release : official journal of the Controlled Release Society* **2014,** *194*, 323-31.
15. Brady, C. E., 3rd; DiPalma, J. A.; Morawski, S. G.; Santa Ana, C. A.; Fordtran, J. S. Urinary excretion of polyethylene glycol 3350 and sulfate after gut lavage with a polyethylene glycol electrolyte lavage solution. *Gastroenterology* **1986,** *90*, (6), 1914-8.
16. Ryan, C. M.; Yarmush, M. L.; Tompkins, R. G. Separation and quantitation of polyethylene glycols 400 and 3350 from human urine by high-performance liquid chromatography. *J Pharm Sci* **1992,** *81*, (4), 350-2.
17. Pelham, R. W.; Nix, L. C.; Chavira, R. E.; Cleveland, M. V.; Stetson, P. Clinical trial: single- and multiple-dose pharmacokinetics of polyethylene glycol (PEG-3350) in healthy young and elderly subjects. *Alimentary pharmacology & therapeutics* **2008,** *28*, (2), 256-65.
18. Donovan, M. D.; Flynn, G. L.; Amidon, G. L. ABSORPTION OF POLYETHYLENE GLYCOL-600 THROUGH POLYETHYLENE GLYCOL-2000 - THE MOLECULAR-WEIGHT DEPENDENCE OF GASTROINTESTINAL AND NASAL ABSORPTION. *Pharmaceutical Research* **1990,** *7*, (8), 863-868.
19. Shaffer, C. B.; Critchfield, F. H. The absorption and excretion of the solid polyethylene glycols; (carbowax compounds). *Journal of the American Pharmaceutical Association. American Pharmaceutical Association* **1947,** *36*, (5), 152-7.

20. Shaffer, C. B.; Critchfield, F. H.; Nair, J. H., 3rd. The absorption and excretion of a liquid polyethylene glycol. *Journal of the American Pharmaceutical Association. American Pharmaceutical Association* **1950,** *39*, (6), 340-4.
21. Volpi, N. Oral bioavailability of chondroitin sulfate (Condrosulf) and its constituents in healthy male volunteers. *Osteoarthritis Cartilage* **2002,** *10*, (10), 768-77.
22. Volpi, N. About oral absorption and human pharmacokinetics of chondroitin sulfate. *Osteoarthritis Cartilage* **2010,** *18*, (8), 1104-5; author reply 1106-7.
23. Qi, Y.; Zhao, G.; Liu, D.; Shriver, Z.; Sundaram, M.; Sengupta, S.; Venkataraman, G.; Langer, R.; Sasisekharan, R. Delivery of therapeutic levels of heparin and low-molecular-weight heparin through a pulmonary route. *Proc Natl Acad Sci U S A* **2004,** *101*, (26), 9867-72.
24. Ott, P. Hepatic Elimination of Indocyanine Green with Special Reference to Distribution Kinetics and the Influence of Plasma Protein Binding. *Pharmacology & Toxicology* **1998,** *83*, 1-48.
25. Hamann, F. M.; Brehm, R.; Pauli, J.; Grabolle, M.; Frank, W.; Kaiser, W. A.; Fischer, D.; Resch-Genger, U.; Hilger, I. Controlled modulation of serum protein binding and biodistribution of asymmetric cyanine dyes by variation of the number of sulfonate groups. *Mol Imaging* **2011,** *10*, (4), 258-69.
26. Ntziachristos, V.; Yodh, A. G.; Schnall, M.; Chance, B. Concurrent MRI and diffuse optical tomography of breast after indocyanine green enhancement. *Proc Natl Acad Sci U S A* **2000,** *97*, (6), 2767-72.
27. Corlu, A.; Choe, R.; Durduran, T.; Rosen, M. A.; Schweiger, M.; Arridge, S. R.; Schnall, M. D.; Yodh, A. G. Three-dimensional in vivo fluorescence diffuse optical tomography of breast cancer in humans. *Opt Express* **2007,** *15*, (11), 6696-716.
28. Hagen, A.; Grosenick, D.; Macdonald, R.; Rinneberg, H.; Burock, S.; Warnick, P.; Poellinger, A.; Schlag, P. M. Late-fluorescence mammography assesses tumor capillary permeability and differentiates malignant from benign lesions. *Opt Express* **2009,** *17*, (19), 17016-33.
29. van de Ven, S.; Wiethoff, A.; Nielsen, T.; Brendel, B.; van der Voort, M.; Nachabe, R.; Van der Mark, M.; Van Beek, M.; Bakker, L.; Fels, L.; Elias, S.; Luijten, P.; Mali, W. A novel fluorescent imaging agent for diffuse optical tomography of the breast: first clinical experience in patients. *Molecular imaging and biology : MIB : the official publication of the Academy of Molecular Imaging* **2010,** *12*, (3), 343-8.
30. Poellinger, A.; Burock, S.; Grosenick, D.; Hagen, A.; Ludemann, L.; Diekmann, F.; Engelken, F.; Macdonald, R.; Rinneberg, H.; Schlag, P. M. Breast cancer: early- and late-fluorescence near-infrared imaging with indocyanine green--a preliminary study. *Radiology* **2011,** *258*, (2), 409-16.
31. Ntziachristos, V.; Chance, B. Probing physiology and molecular function using optical imaging: applications to breast cancer. *Breast cancer research : BCR* **2001,** *3*, (1), 41-6.
32. Davis, S. C.; Pogue, B. W.; Dehghani, H.; Paulsen, K. D. Tissue drug concentration determines whether fluorescence or absorption measurements are more sensitive in diffuse optical tomography of exogenous contrast agents. *Appl Opt* **2009,** *48*, (10), D262-72.
33. Collettini, F.; Martin, J. C.; Diekmann, F.; Fallenberg, E.; Engelken, F.; Ponder, S.; Kroencke, T. J.; Hamm, B.; Poellinger, A. Diagnostic performance of a Near-Infrared Breast Imaging system as adjunct to mammography versus X-ray mammography alone. *European radiology* **2012,** *22*, (2), 350-7.
34. Li, X.; Chance, B.; Yodh, A. G. Fluorescent heterogeneities in turbid media: limits for detection, characterization, and comparison with absorption. *Appl Opt* **1998,** *37*, (28), 6833-44.
35. Adams, A.; Mourik, J. E.; van der Voort, M.; Pearlman, P. C.; Nielsen, T.; Mali, W. P.; Elias, S. G. Estimation of detection limits of a clinical fluorescence optical mammography system for the near-infrared fluorophore IRDye800CW: phantom experiments. *Journal of biomedical optics* **2012,** *17*, (7), 076022.
36. Frangioni, J. V. New technologies for human cancer imaging. *Journal of Clinical Oncology* **2008,** *26*, (24), 4012-4021.
37. Zhang, L.; Bhatnagar, S.; Deschenes, E.; Thurber, G. M. Mechanistic and quantitative insight into cell surface targeted molecular imaging agent design. *Scientific reports* **2016,** *6*, 25424.
38. Bhatnagar, S.; Deschenes, E.; Liao, J.; Cilliers, C.; Thurber, G. M. Multichannel Imaging to Quantify Four Classes of Pharmacokinetic Distribution in Tumors. *Journal of pharmaceutical sciences* **2014,** *103*, (10), 3276-3286.
39. Dayton, P. A.; Pearson, D.; Clark, J.; Simon, S.; Schumann, P. A.; Zutshi, R.; Matsunaga, T. O.; Ferrara, K. W. Ultrasonic analysis of peptide- and antibody-targeted microbubble contrast agents for molecular imaging of alphavbeta3-expressing cells. *Mol Imaging* **2004,** *3*, (2), 125-34.
40. Waldeck, J.; Hager, F.; Holtke, C.; Lanckohr, C.; von Wallbrunn, A.; Torsello, G.; Heindel, W.; Theilmeier, G.; Schafers, M.; Bremer, C. Fluorescence reflectance imaging of macrophage-rich atherosclerotic plaques using

an alphavbeta3 integrin-targeted fluorochrome. *Journal of nuclear medicine : official publication, Society of Nuclear Medicine* **2008,** *49*, (11), 1845-51.
41. Taherian, A.; Li, X.; Liu, Y.; Haas, T. A. Differences in integrin expression and signaling within human breast cancer cells. *BMC Cancer* **2011,** *11*, 293.
42. Takayama, S.; Ishii, S.; Ikeda, T.; Masamura, S.; Doi, M.; Kitajima, M. The relationship between bone metastasis from human breast cancer and integrin alpha(v)beta3 expression. *Anticancer research* **2005,** *25*, (1A), 79-83.